



DYNAMICS OF PITCHING CONTROL MECHANISM
OF SMALL PROPELLER-TYPE WIND MACHINES

ATEF M.A. HASSANEIN[✱], FATHY A.A. EID^{✱✱}

ABSTRACT

The paper is aiming at exploring the area of pitch control type of regulation used in small propeller-type wind machines. To cover the lack of published information about the real design criteria of such type of regulation, this work is carried out to develop the pertaining theoretical database. The paper investigates the dynamic performance of the centrifugally-activated pitch control mechanisms widely-used in wind machines. A typical pitching mechanism is chosen to be the subject of analysis; namely the crank-slider-crank mechanism which is centrifugally-activated by hub-mounted fly weights. The kinematic and dynamic characteristics of the candidate system are fully analysed. The results are presented in a group of charts in terms of the system dimensionless design-parameters, best suiting the engineers for design purposes.

1. INTRODUCTION

Pitching is that form of action that causes a change of the setting angle of the propeller blade (or of part of it). As a consequence of that, the angle of attack of each airfoil section along the blade, changes with respect to the relative wind speed. This change has a direct influence on the speed of rotation and/or the power extracted from the wind. The propeller-type small wind energy conversion systems (PT-SWECS) considered in this paper, are normally used for electricity generation. Depending upon the specific application, pitch control in PT-SWECS is used to perform one or more of the following requirements [1-5]:

✱ Associate Professor, Dept. of Aeronautics, Faculty of Engineering, Cairo University, Giza, Egypt.

✱✱ Colonel Engineer, Head of Quality Dept., EAF Helwan O/H Depot, Ph.D. Student, Dept. of Aeronautics, Cairo Univ.



- o Self starting of the wind machine.
- o Optimum matching between the wind rotor and the generator used.
- o Limiting the wind machine power-output in the range of operation between the rated wind speed and the cut-out wind speed.
- o Keeping constant rotational speed through the whole operation range of the PT-SWECS while maintaining an optimum output for any particular tip speed ratio.

Reviewing the commercially-available PT-SWECS, [6], it has been found that blade pitching is a practically proved concept for control. Blade pitching is adopted for control in more than 70 % of the currently produced types of PT-SWECS, [5] & [6]. Furthermore, in all of these machines, the pitch-change mechanism is centrifugally-activated via the centrifugal action of masses rotating with the rotor. The objective of this paper is to study and analyse the so-called hub-mounted fly-weight pitch control mechanism. The paper lays down the governing relations required for designing and/or predicting the performance of the mechanism.

2. KINEMATICS OF THE SYSTEM

The investigated pitch-control mechanism is a typical one which comprises three main components, as shown in Fig.(1). These are: the speed sensor, the output transmitter, and the transmission mechanism. The system contains as much of this mechanism, as the number of the rotor blades.

The pitching mechanism is equivalent to the planar crank-slider-crank mechanism shown in Fig.(2). When the mass is affected by the centrifugal force, it is forced to move in an arc of a circle having the center at point P. Crank 1 will follow the mass movement. Consequently, crank 2 will be forced to move about the hinge P₀, and point P₃ will move in a circular path of center at P₀. The slider will slide on crank 1 upward/downward, depending on the direction of motion. The slider translatory motion of Fig.(2), is equivalent to the motion of the slot of the mass lever relative to the pin of the output transmitter of Fig.(1). More details on equivalent mechanisms are provided in [7].

2.1 GEOMETRY OF MOTION

Referring to Fig.(3), and assuming that the mass lever is so designed with 90° angle between its legs, the following relations can be deduced, [6],:

$$X_1 = \sqrt{a^2 + R^2 + 2 a R \sin \psi} \quad (1)$$

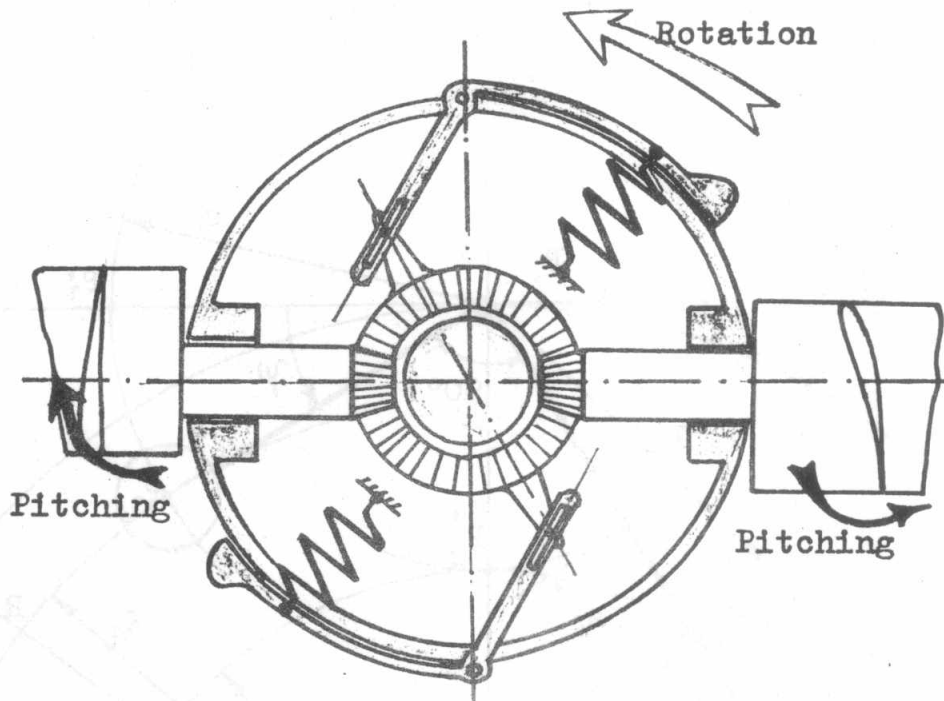


Fig.(1): Schematic Diagram of the Investigated Hub-Mounted Fly-Weight Pitching Mechanism

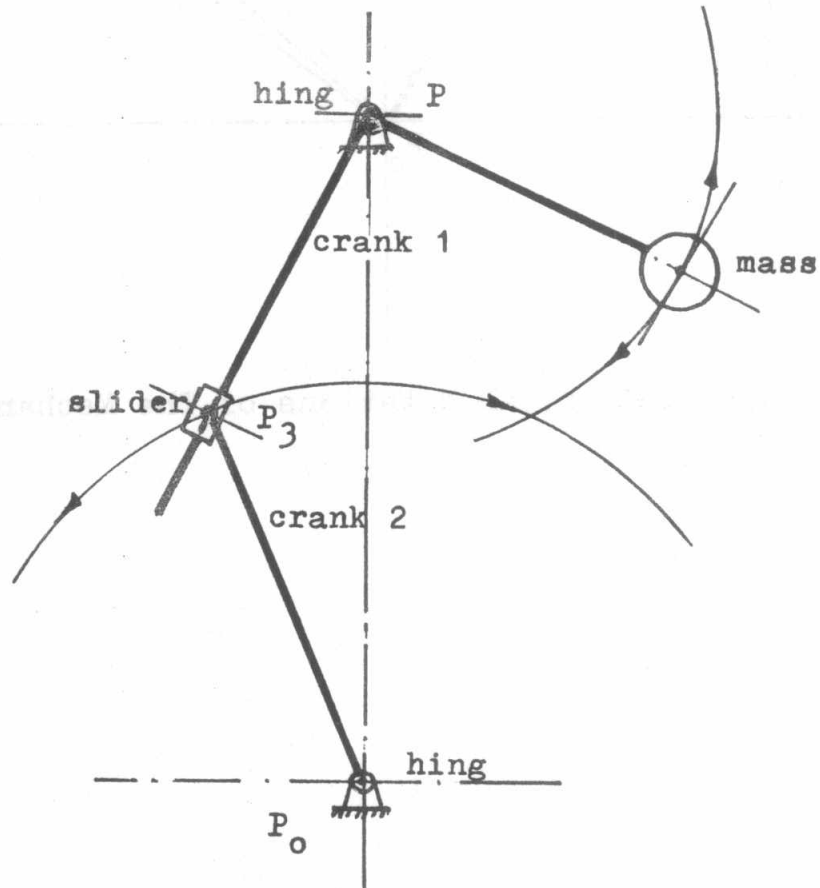


Fig.(2): The Planar Crank-Slider-Crank

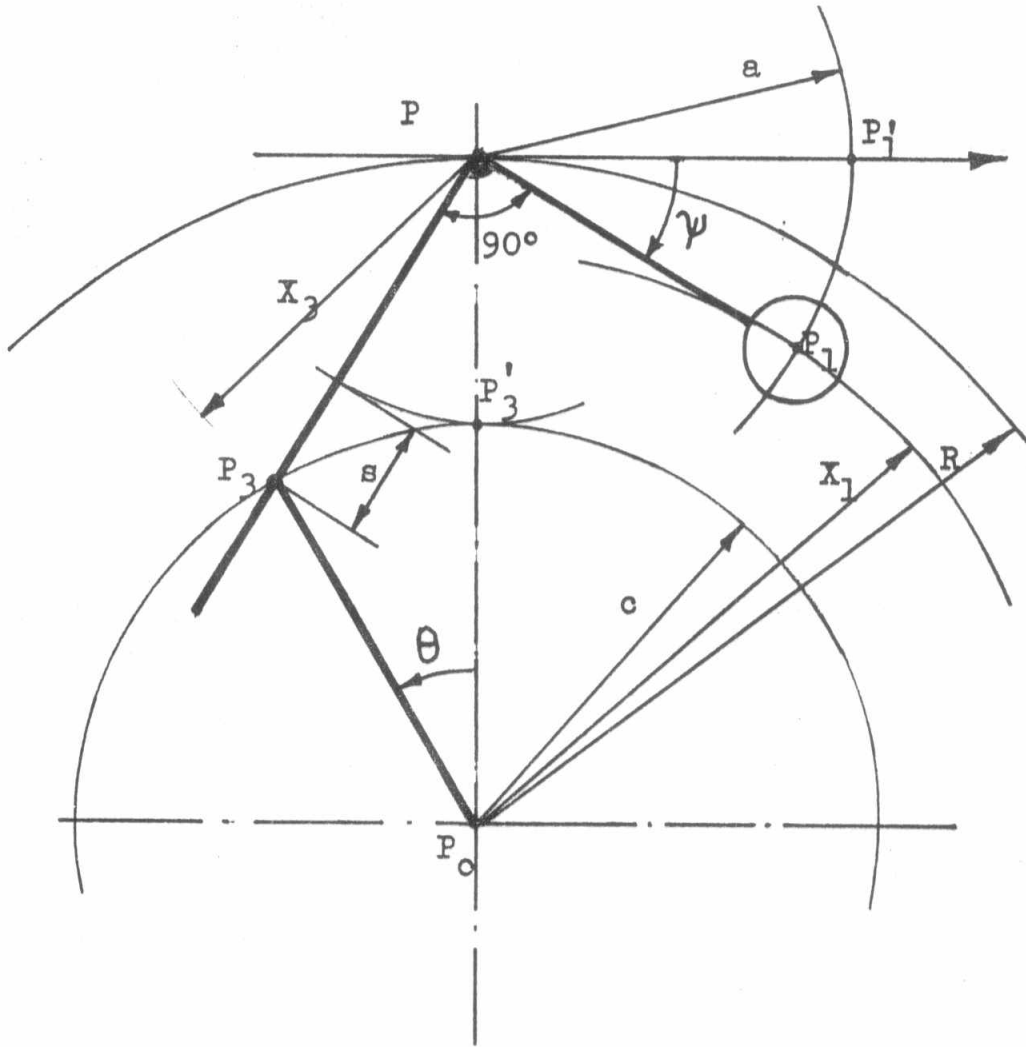


Fig.(3): Geometrical Notations of The Mechanism



6

$$X_3 = c (\sin \theta / \sin \psi) \quad (2)$$

$$c \cdot \sin(\psi + \theta) = R \cdot \sin \psi \quad (3)$$

$$s = X_3 - R + c \quad (4)$$

The above relations can be expressed, more conveniently, in dimensionless form by introducing the geometrical parameters A & C, where A is the fly-weight arm ratio and C is the blade driving-arm ratio; defined by:

$$A = a/R \quad (5)$$

$$C = c/R \quad (6)$$

Equations (1) to (4) become:

$$\bar{X}_1 = \sqrt{1 + A^2 + 2 A \sin \psi} \quad (7)$$

$$\bar{X}_3 = C \sin \theta / \sin \psi \quad (8)$$

$$\sin \psi = C \sin(\psi + \theta) \quad (9)$$

$$S = \bar{X}_3 + C - 1 \quad (10)$$

where:

$$\bar{X}_1 = X_1/R, \quad \bar{X}_3 = X_3/R, \quad \text{and} \quad S = s/R \quad (11)$$

2.2 CRITERION OF MECHANISM INTEGRITY

Fig.(2) shows that crank 1 can drive crank 2 until they are at right angle. This condition occurs on both sides of PP^o. This is a criterion that puts a limit on the maximum possible movement of the fly-weight mass with the mechanism still having its integrity. At the limiting positions, the following relation is valid:

$$\sin \psi = \pm C \quad (12)$$

It follows that the criterion of system integrity is:

$$- C \geq \sin \psi \geq + C \quad (13)$$

The relations defining the geometry of motion of the mechanism, are presented in the form of dimensionless-parameters charts on Figs.(4) to (7). It is evident that for small values of ψ , the mechanism movement is approximately linear.

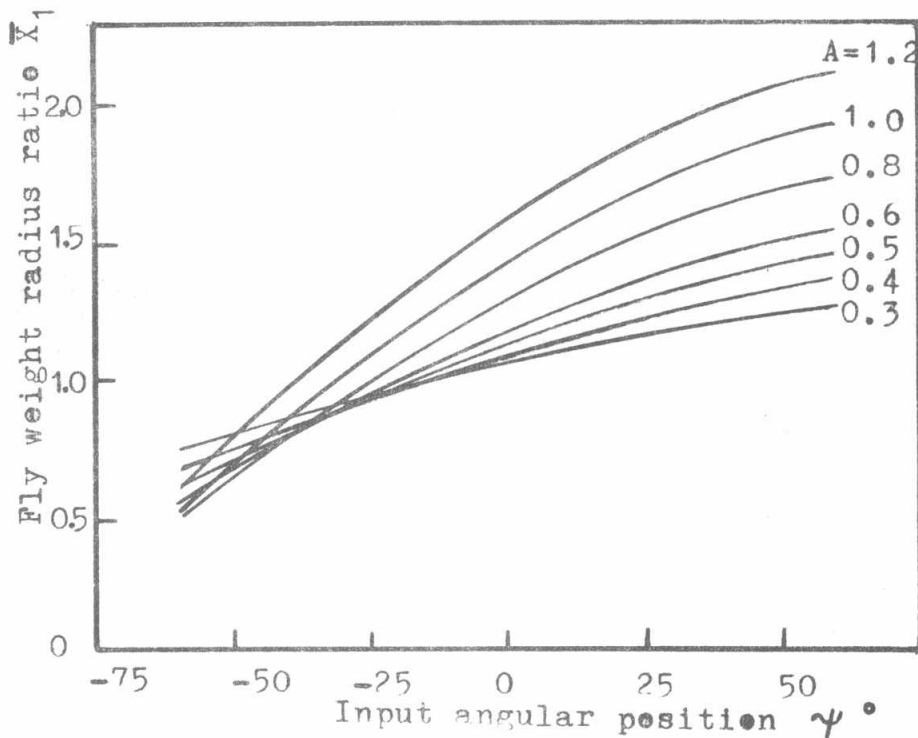


Fig.(4): Variation of the Radius Ratio \bar{X}_1 against Input Angular Position ψ

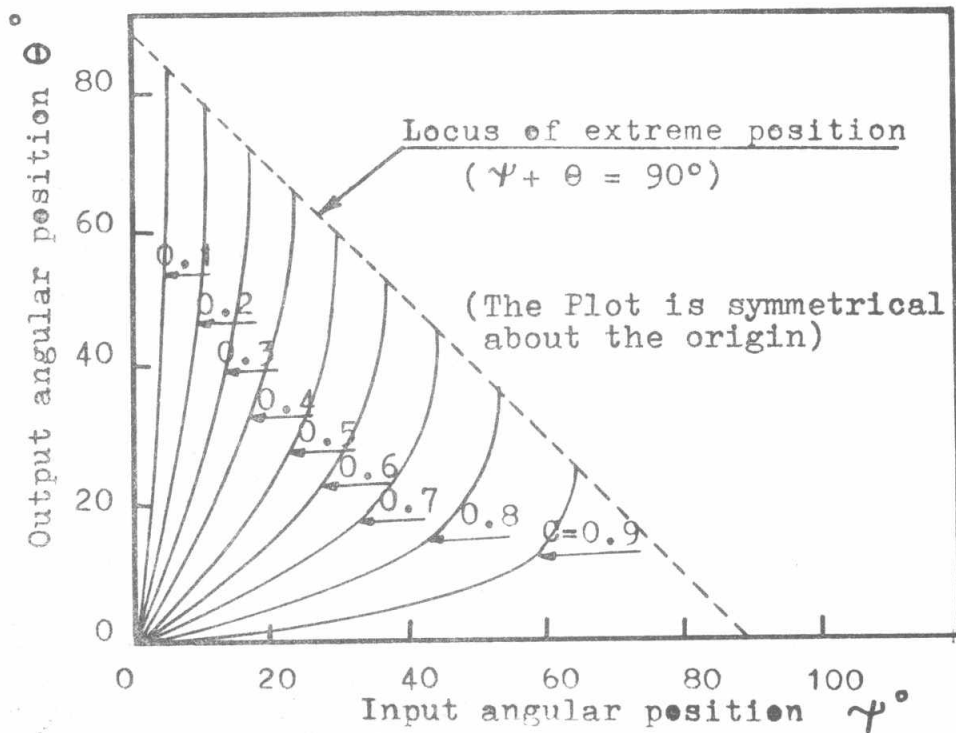


Fig.(5): Variation of the Output Angular Position θ against Input Angular Position ψ



6

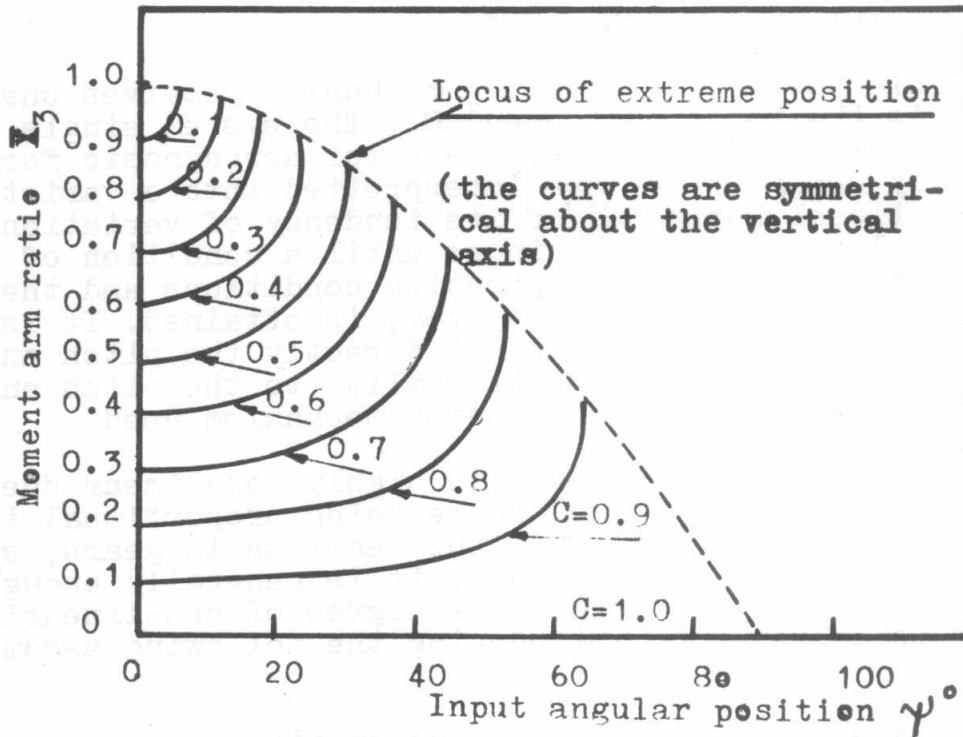


Fig.(6): Variation of the Moment-Arm Ratio \bar{X}_3 against Input Angular Position ψ

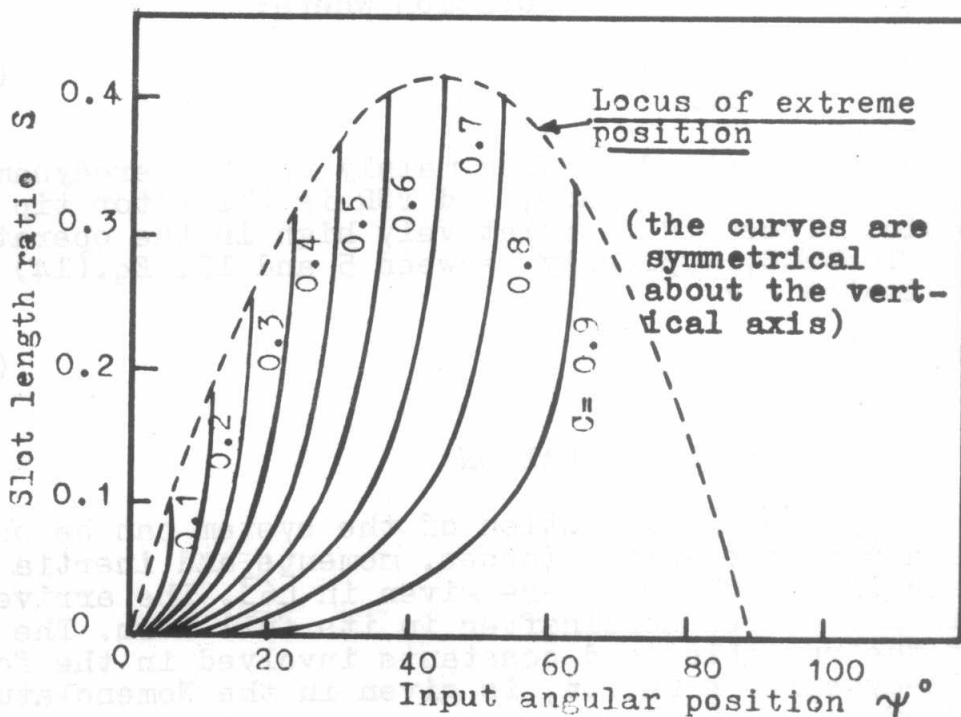


Fig.(7): Variation of the Slot-Length Ratio S against Input Angular Position ψ



3. DYNAMICS OF THE SYSTEM

As a control system, the pitching mechanism receives one input which is the rotational speed Ω . The system single output is the setting angle θ . As the rotor aerodynamic forces consequently change, they are interpreted into a variation of the rotational speed and/or its tendency of variation. This closed loop process continues until a condition of equilibrium, depending upon the operation conditions and the inherent characteristics of the system, is attained. It is worth mentioning that angle θ is not directly the pitch angle. However, it is in direct proportionality to the pitch angle, in a way depends on the transmission mechanism used.

The system under investigation, is highly non-linear due to: its geometry, the centrifugal force being proportional to the square of the rotational speed, the backlash in gears, spring hysteresis, ... etc. Nevertheless, it is generally enough for practical application to limit the degree of non-linearity, [8]. This is achieved by introducing the following assumptions:

- o The activated mass is concentrated at its C.G.
- o The spring force-deflection relation is linear.
- o The line of action of the spring force is always radial.
- o The damping in the system is of the viscous type, i.e., it is proportional to the angular speed $\dot{\theta}$.
- o The blade pitching-moment is transferred as a balancing moment M about the axis of rotation where:

$$M = N \Omega^2 R^2 \left(1 + \frac{1}{(\text{TSR})^2} \right) \quad (14)$$

where N is a constant depending mainly on the aerodynamic characteristics of the blade, and TSR is the rotor tip speed ratio. Since TSR is relatively high in the operation range of PT-SWECS, typically between 5 and 15, Eq.(14) can be approximated to:

$$M \cong N \Omega^2 R^2 \quad (15)$$

3.1 THE GOVERNING EQUATION

The equation governing the motion of the system can be obtained by balancing the acting forces, moments and inertia terms. The details of this step are given in [6]. The arrived-at equation is introduced hereinafter in its full form. The definition of the variables and constants involved in the following system-dynamics equation, is given in the Nomenclature at the end of the paper.



$$\begin{aligned}
 & (C/\bar{X}_3) \cos(\psi + \theta) \left[(J/mR^2)(\bar{X}_3^2/C^2) - 1 \right] \theta'' + \left[(1-C^2) \sin\psi/\bar{X}_3^3 \right] \theta'^2 \\
 & + \left[(\lambda/ma^2)(\bar{X}_3/C) \cos(\psi + \theta) \right] \theta' + (M/ma^2)(\bar{X}_3/C) \cos(\psi + \theta) \\
 & + (K/mA)(1 - \bar{L}/\bar{X}_1) \cos\psi = \left[(A + \sin\psi)/A \right] \Omega' + (\cos\psi/A) \Omega^2
 \end{aligned} \tag{16}$$

The above equation is non-linear, second-order, second-degree ordinary differential equation with time-dependent coefficients. The input function Ω appears in the governing equation in two forms; its square (Ω^2) and its rate of change (Ω'). Thus the system is expected to respond either to the rotational speed change or to its tendency to change, or to both of them. This is a favourable characteristics, [8] to [10]. In what follows, the dynamic analysis of the system is performed via an exact steady state analysis only. A transient-response analysis, not included in the present paper because of the limited space, is provided in [6].

3.2 EXACT STEADY STATE ANALYSIS

The steady state, which is alternatively called the equilibrium running state, is obtained, as described in [11], by setting θ'' , θ' and Ω' equal to zero in Eq.(16). Doing so, the following expression, defining the state of steady running of the system, is obtained:

$$\Omega = \sqrt{\frac{(1 - \bar{L}/\bar{X}_1)}{\left[1 - H_1(\bar{X}_3/AC) [\cos(\psi + \theta) / \cos\psi] \right]}} \tag{17}$$

By examining the above equation, and in the light of that for practical application, \bar{L} is generally less than unity and \bar{X}_1 is more than unity, it can be seen that the system cannot physically exist unless the following expression is satisfied:

$$H_1 < (AC/\bar{X}_3) [\cos\psi / \cos(\psi + \theta)] \tag{18}$$

This criterion puts an upper limit to the design parameter H_1 (i.e., the ratio N/m) which must not be exceeded at any operating point of the mechanism defined by angle ψ and its geometry. The system existence criterion defined by the inequality in Eq.(18), is represented in parametric non-dimensional chart in Fig.(8). It is readily apparent that the above criterion is a direct correlation between the blade characteristics defined by N and the system activation element defined by the mass m . The system can be reduced to a simple centrifugal speed sensing device by setting $H_1=0$. As it will be shown later, the ratio H_1 is almost the major factor affecting the system performance.



Going further, the system steady state running characteristics are fully defined, [11] & [12], by defining: the input/output relation $\bar{\Omega} - \theta$ and the input/gain relation $\bar{\Omega} - \bar{G}$. The first one is defined by Eq.(17), while the second is simply obtained by differentiating Eq.(17), giving:

$$\bar{G} = d\theta/d\bar{\Omega} \quad (19)$$

$$= \frac{4 \cos \psi \cdot (1 - \bar{L}/\bar{X}_1)}{K_1 \bar{\Omega} [K_7(1 - \bar{\Omega}^2) - (\bar{L}/\bar{X}_1)(K_7 - 2A \cos^2 \psi / \bar{X}_1^2)]} \quad (20)$$

where:

$$K_1 = (C/\bar{X}_3) \cos(\psi + \theta) \quad (21)$$

$$K_7 = (\sin 2\psi / \bar{X}_3 K_1^2) - 2 \sin \psi \quad (22)$$

Figs.(9) and (10) are examples for the steady state characteristics defined by Eqs.(17) and (20), respectively. The tremendous effect of the design parameter H_1 on the system behaviour, is quite clear in the two figures.

Depending upon the values of A, C, and \bar{L} , the characteristic line for a certain value of H_1 takes one of the shapes shown on Fig.(11) or Fig.(12). The operating line shown in Fig.(11) is a continuous function starts at P_1 and ends at P_2 after reaching a peak where $\bar{\Omega} = \bar{\Omega}_{\max}$ and $\theta = \theta(\bar{\Omega}_{\max})$. Fig.(12) shows the case when the operating line is not a continuous function, and where a phenomenon of branching occurs at the point P_3 where $\bar{\Omega} = 0$ and $\theta = \theta_B$.

Since the negative gain regimes imply some kind of instability, [9] & [10], it is recommended to limit the operating regime of the system to be within the positive gain region. In the case of Fig.(11), the operating regime is defined by: $\theta \leq \theta(\bar{\Omega}_{\max})$, whilst in Fig.(12) it is defined by $\theta_B \leq \theta \leq \theta(\bar{\Omega}_{\max})$.

Since the branching phenomenon is not a desirable one, it is also recommended to keep a certain correlation between the parameters A, C, and \bar{L} , to avoid the occurrence of this phenomenon. To define this correlation, we proceed as follows:

The branching point is always at $\bar{\Omega} = 0$. At this point, $\theta = \theta_B$ where $\theta_B \geq$ the minimum physical θ . From Eq.(17), $\bar{\Omega} = 0$ when

$$1 - \bar{L}/\bar{X}_1 = 0, \text{ which means (using Eq.(7)) that } \sin \psi (\bar{\Omega} = 0) = (\bar{L}^2 - A^2 - 1)/2A. \text{ Provided that } \psi (\bar{\Omega} = 0) \geq \psi_{\min} \text{ and since}$$

$\sin \psi_{\min} = -C$, then the branching phenomenon will occur if

$$\bar{L}^2 \geq 1 + A^2 - 2AC. \text{ This means that the necessary and suffic-}$$

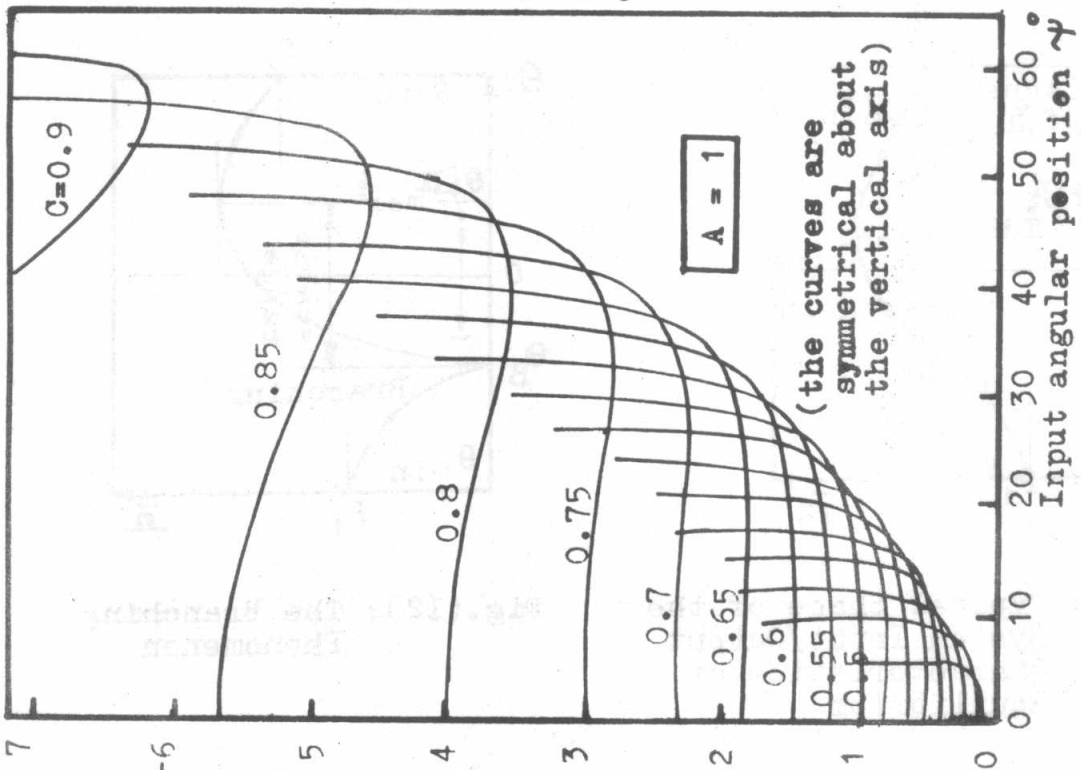


Fig.(8): The System Existence Criterion H_1 (per) against Input Angular Position ψ

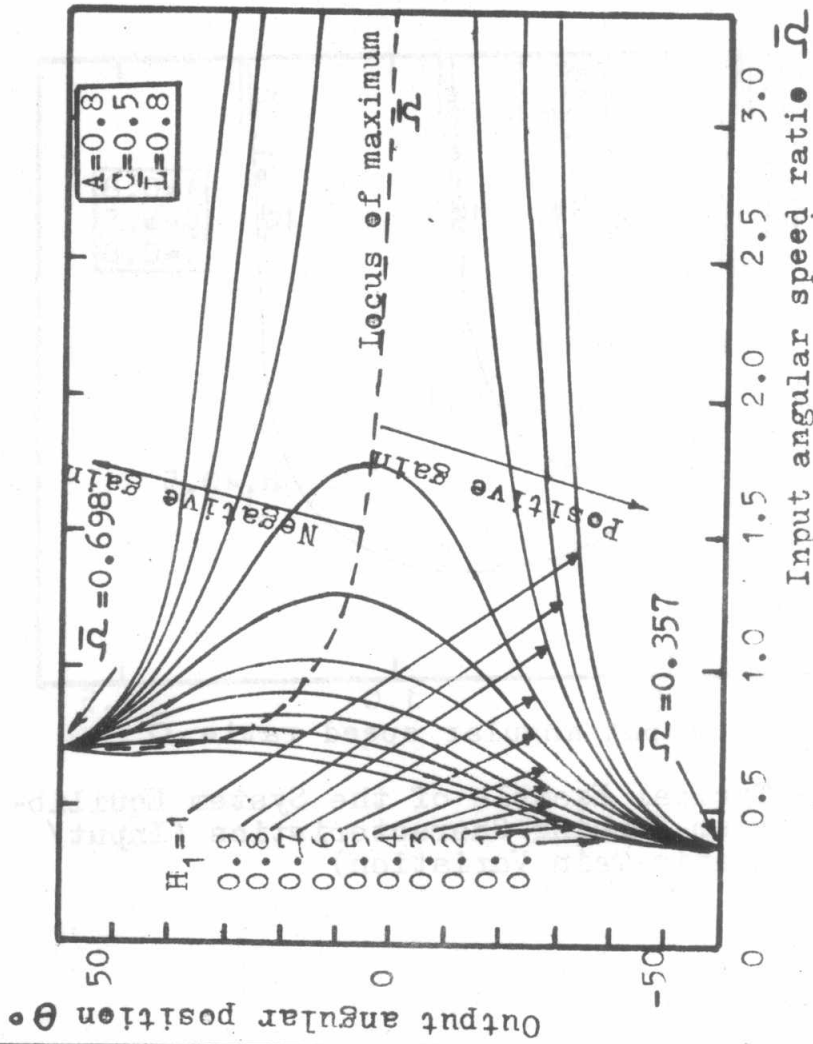


Fig.(9): Typical Example of the System Equilibrium-Running Characteristics (Input/Output Variation)

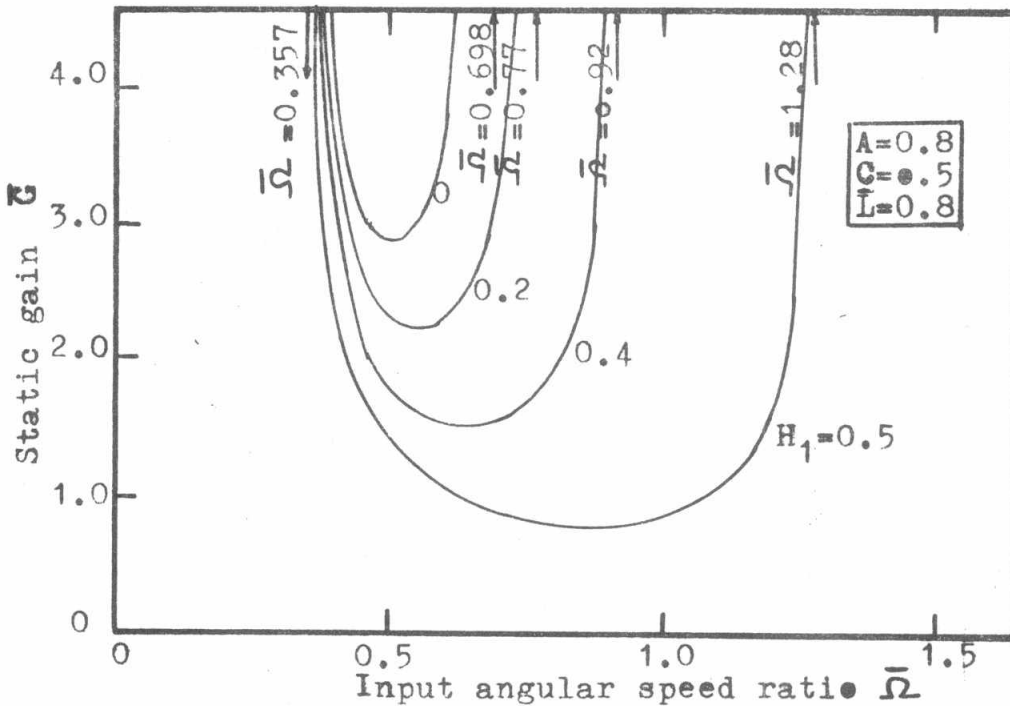


Fig.(10): Typical Example of the System Equilibrium-Running Characteristics (Input/Static-Gain Variation)

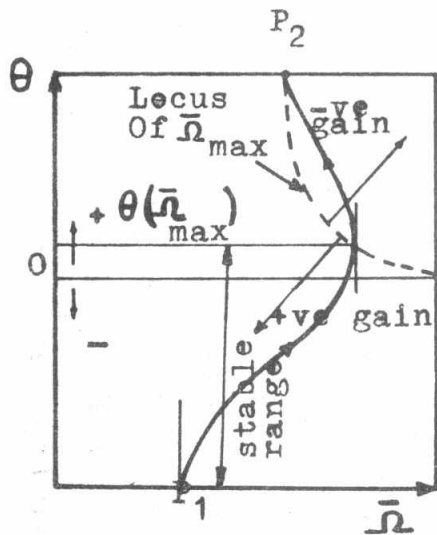


Fig.(11): Typical Shape of the System Input/Output Characteristics at Equilibrium

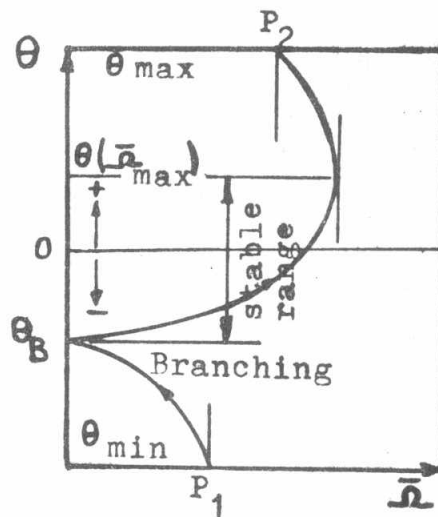


Fig.(12): The Branching Phenomenon



ient condition to avoid the branching phenomenon is given by:

$$\bar{L} < 1 + A^2 - 2AC \quad (23)$$

The chart shown in Fig.(13) is prepared on the basis of the above correlation to guide the proper choice of A, C, and \bar{L} . The other border of the positive gain regime is defined by $\bar{\omega} = \bar{\omega}_{\max}$. The locus of $\bar{\omega}_{\max}$ can be found from Eq.(20) by setting $\bar{\omega}_{\max} = \infty$, which yields:

$$\bar{\omega}_{\max} = \left[1 - (\bar{L}/\bar{X}_1) \left(1 - \frac{2 A \cos^2 \gamma}{K_7 \bar{X}_1^2} \right) \right] \quad (24)$$

Fig.(14) presents a typical example of such locus.

4. CONCLUSIONS

The design and performance criteria of a typical pitch-control mechanism, have been studied. The kinematic and dynamic characteristics of the hub-mounted fly-weights, centrifugally activated, crank-slider-crank mechanism, are fully analysed. The analysis provided in this paper constitutes an adequate base for the designer to choose the system parameters. Depending upon the aimed-at performance of the system, and using the charts and information provided by this paper, it is possible to design and synthesize a system that will perform as required. Moreover, the performance of an existing system can be improved statically and dynamically.

5. REFERENCES

1. Golding, E.W. and Harris, R.I., "The Generation of Electricity by Wind Power", E. and F.N. Spon LTD, London (1976).
2. Lumsdaine, E., "Review of Status of the Potential of Wind Energy", UNESCO-Consultant Report, Cairo University, Giza, Dec. (1979).
3. Research and Development - War Production Board, "Final Report on Wind Turbines", Research Report Pb 25370, Chapter III, Washington D.C (1964).
4. Park, J., "The Wind Power Book", Cheshire Books, Palo Alto, California (1981).
5. Hunt, V.D., "Wind Power - A Handbook on Wind Energy Conversion Systems", Van Nostrand Reinhold Company, New York, (1981).
6. Eid, F.A.A. (The second author of the present paper), "Dynamics of Pitching Control Mechanism of Small Propeller Wind Machines", M.Sc. Thesis, Dept. of Aeronautics, Faculty of Engineering, Cairo University, Giza (1985).
7. Dijkman, E.A., "Motion Geometry of Mechanisms", Cambridge University Press (1976).

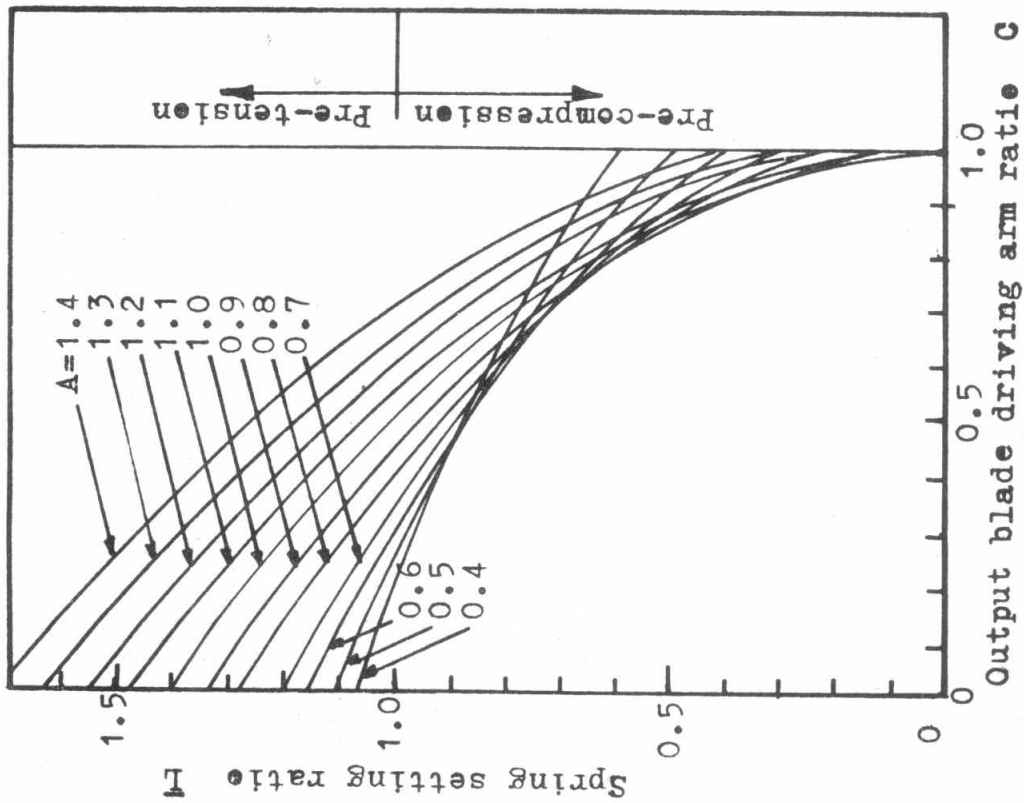


Fig.(13): Chart governing the Choice of A, C, and L to avoid the Branching

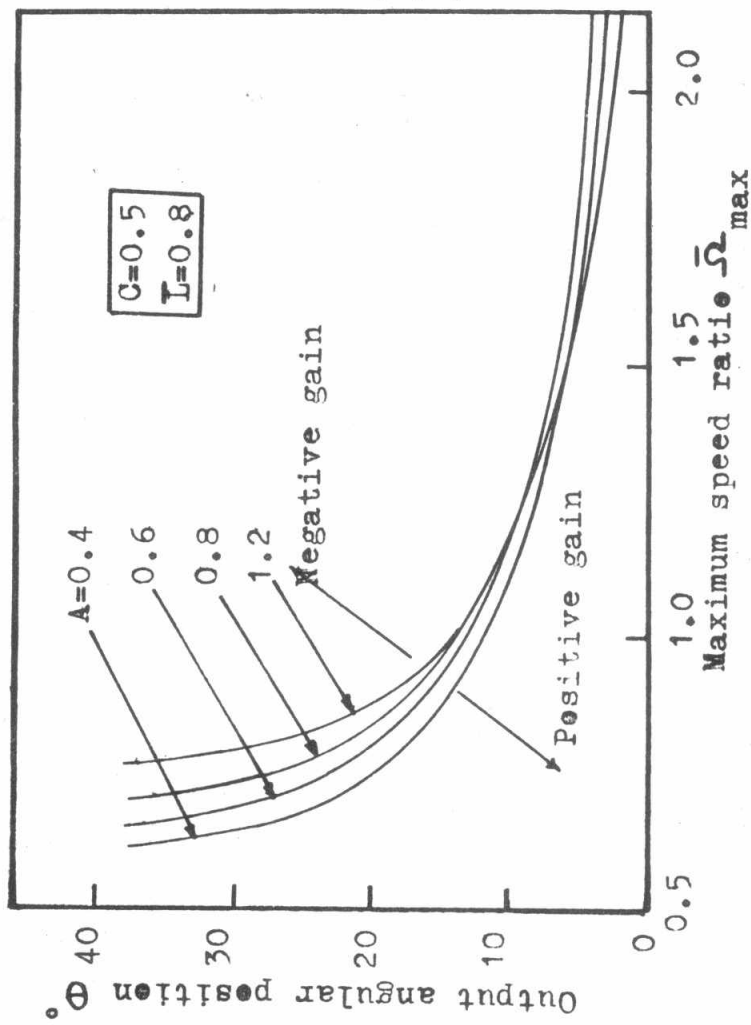


Fig.(14): Typical Example of the System $\bar{\Omega}_{max}$ Locus



8. Shinnars, S.M., "Modern Control System Theory and Application", Addison-Wisley Publishing Company.
9. Dransfield, P., "Engineering Systems and Automatic Control", Printice-Hall of India (1974).
10. Truxal, J.G., "Automatic Feedback Control System Synthesis", McGraw-Hill, (1955).
11. Parnaby, J., "Dynamic and Steady State Characteristics of A Centrifugal Speed Governor", The Engineer, Nov.(1964).
12. Mohamed, N.A., "Comparative Study of Centrifugal Speed-Sensing Devices", M.Sc. Thesis, Dept. of Aeronautics, Faculty of Engineering, Cairo University, Giza (1967).

6. NOMENCLATURE

A	fly-weight arm ratio; Eq.(5)
a	length of fly-weight arm; Fig.(3)
C	moment-arm ratio; Eq.(6)
c	arm of driving output moment; Fig.(3)
\bar{G}	dimensionless static gain of system; $\bar{G}=G/\sqrt{K/m}$, where G is the static gain
H_1	pitching-moment ratio; $H_1=N/m$
J_1	equivalent polar moment of inertia of driven masses
K	spring force/deflection constant of proportionality
K_1	system parameter; Eq.(21)
$\frac{K_1}{L}$	system parameter; Eq.(22)
$\frac{L}{R}$	spring-setting ratio; $L=L/R$, where L is component of spring-setting in the radial direction
m	mass of the whole centrifugally-activated fly-weight
M	equivalent blade pitching-moment transferred to the rotor axis; Eqs.(14) & (15)
N	pitching-moment constant of proportionality; Eq.(14)
PT-SWECS	propeller-type small wind energy conversion system
R	characteristic hub-radius of mechanism; Fig.(3)
S	slot-length ratio; Eq.(11)
s	slot length; Figs.(2) & (3)
TSR	tip speed ratio of rotor
$\frac{x_1}{L}$	radial distance of fly-weight; Fig.(3)
$\frac{x_1}{L}$	dimensionless x_1 ; Eq.(11)
$\frac{x_3}{L}$	distance between pivot P and contact point P_3 on slot; Figs.(2) & (3)
$\frac{x_3}{L}$	dimensionless x_3 ; Eq.(11)
λ	system viscous-damping coefficient
ψ	angular position of fly-weight arm; Fig.(3)
θ	angular-position output of mechanism; Fig.(3)
θ_B	value of θ at branching point; Fig.(12)
$\dot{\theta}$	rate of change of θ with time
$\dot{\theta}'$	rate of change of θ' with time
Ω	rotor speed of rotation; Fig.(1)
$\dot{\Omega}$	rate of change of Ω with time
$\bar{\Omega}$	dimensionless Ω ; $\bar{\Omega} = \Omega / \sqrt{K/m}$

